NUMERICAL INVESTIGATION OF HYDRODYNAMIC PERFORMANCE OF MARINE PROPELLER

Md. Shahjada Tarafder[1], Imdadul Haque[2], Md. Zahidul Islam laku[3], Md. Assaduzzaman[4]

[1]Department of Naval Architecture and Marine Engineering.
Bangladesh University of Engineering and Technology, Dhaka, Bangladesh.
E-mail:

[2]Department of Naval Architecture and Marine Engineering.
Bangladesh University of Engineering and Technology, Dhaka, Bangladesh.
E-mail:

[3]Department of Naval Architecture and Marine Engineering.
Bangladesh University of Engineering and Technology, Dhaka, Bangladesh.
E-mail: zahidlaku72@gmail.com

[4]Department of Naval Architecture and Marine Engineering.
Bangladesh University of Engineering and Technology, Dhaka, Bangladesh.
E-mail:

ABSTRACT

An efficient and optimized propeller can reduce ship operating costs substantially. The recent development of Computational Fluid Dynamics (CFD) has significant impact on initial stage of propeller design. Being motivated by the success of a CFD approach known as Reynolds Averaged Navier-Stokes Equation (RANSE) in solving many hydrodynamic problems, this paper explores the use of RANSE solver to estimate propeller open water characteristics. Multiple RANSE solvers can be used for CFD simulation. Among these $k-\epsilon$ turbulence model is used for its better performance on propeller analysis. Numerical results are compared with the results obtained from well-established polynomial regression formulae of Wageningen-B series propeller. Comparison shows an error of less than 5% for most of the cases. The same propeller is numerically analyzed again after fitting a 19A duct on it. To achieve optimal performance space between duct and propeller blade tip is kept as small as possible. Grid independence test is done in both cases for a more accurate estimation within a particular time frame. Mesh sensitivity analysis is carried out in this paper based on thrust and torque coefficients. This paper shows that both the conventional and ducted propeller systems have the highest efficiency of 60% but at different speeds. The ducted propeller system gives better performance up to advance coefficient $J = 0.48$.

Keywords: *Computational fluid dynamics; propeller analysis; ducted propeller; RANSE solver*

1.0 INTRODUCTION

The present maritime industry is substantially more competitive than it was before [14]. To survive in the industry by achieving high speed and low power consumption an optimized and efficient propeller design is far more important now. Traditional propeller design is experiment-based. This requires a higher cost and a significant amount of time. But nowadays with the rapid development of computer tools, many hydrodynamic problems can be readily solved using Computational Fluid Dynamics (CFD) techniques. Within CFD method, there are many different approaches of CFD applications on estimating propeller open water characteristics. These are Blade-Element Theory, Lifting Line Theory, Surface Panel methods, Boundary Element Methods and Reynolds Averaged Navier-Stokes Equation (RANSE) [17]. RANSE is the most popular among these because it is more similar to actual fluid flow around the propeller. But it requires higher cost and computational time. In recent times, with the advancement of computer technology there is a significant increase in computational power. This makes the RANSE simulation to be the preferred practice at the initial stage of propeller design.

Due to the great promise RANSE method has shown, researchers and authors have frequently used it in recent times to estimate propeller open

water characteristics. Funeno [7] simulated fluid flow around a highly skewed propeller via unstructured mesh. For steady and unsteady flow, simulated results have good correspondence with experimental data. But this method was complicated and time consuming. Marti nez-Calle et al. [13]studied numerical analysis of propeller via $k-\epsilon$ turbulence method in steady state condition. The results were acceptable but there was approximately 30% error in the prediction of the torque coefficients. Watanabe et al. [25] simulated propeller via $k-\omega$ turbulence model in open water and steady state condition. Propeller symmetry was used in this study and only one blade was simulated, comparing to the experimental test there was 15% of error. Saha et al. [20] performed CFD simulation of a Wageningen B-series propeller and obtained lowest percentage of error in K_T and K_Q was 13% compared with the results obtained from the empirical formulae. Trejo et al. [23] performed numerical analysis of marine propeller using ANSYS CFX 11. Full model of the propeller and only one blade of that propeller was simulated respectively. Obtained results has less than 10% error in estimating thrust and torque coefficient. Mossad et al. [15] provided a complete guideline for geometry generation, boundary conditions, setup, simulation and problems to achieve accurate results using CFD for marine propeller analysis. Both $k-\epsilon$ and $k-\omega$ turbulence model were used in this study. It concluded that $k-\epsilon$ sometimes overestimates the propeller open water characteristics. Prokash and Nath [18] investigated four bladed Wageningen B-series propeller and numerically analyzed using unstructured mesh. Parra [16] indicated no correlation in the differences between RANS analysis and Lifting Line Theory and obtained good results even for high advance ratio (up to $J=1$). Elghorab et al. [5] suggested suitable mesh model through grid convergence test.

Bahatmaka et al. [1] investigated KP505 propeller by SST $k-\omega$ model and obtained best mesh configuration through grid convergence test which results in less than 2% error in thrust. Triet et al. [24] carried out mesh sensitivity analysis based on Y+ value and suggested that $k-\epsilon$ turbulence model gives quite good result except at high advance ratio (above $J=0.7$). Kolakoti et al. [11] performed CFD analysis of bare hull of a ship, open water analysis of a controllable pitch propeller and flow characteristics of that propeller attached with the same hull. Numerical results obtained from this study has 4% and 14% error in thrust and torque coefficient respectively in the operational regime of the propeller. Fitriadhy et al. [6] performed CFD analysis of propeller for different number of blades and found that three blade propellers are most efficient within the advance coefficient ranging between 0.8 to 0.9. Boumediene et al. [2] studied the flow around Seiun Maru highly skewed marine propeller in both steady and unsteady case obtained average error percentage of 4.18% and 6.04% for thrust and torque coefficients respectively. In unsteady case they suggested to bring the inlet boundary closer to the propeller. Harish et al. [9] performed static analysis on a 4-bladed B-series propeller which was modelled using PropCad. Analysis was done for different materials (aluminum, R glass, S2 glass, carbon epoxy) and results showed that aluminum propeller provides minimum deformation. DurgaNeeharika and Babu [4] found that metallic propellers can be replaced by composite propellers due to enhanced performance within the operating range. Shreyash et al. [21] found that low weight blade can be designed and manufactured with strong load carrying capacity and increase in efficiency of marine propeller on replacement with composite material by reducing its without compromising its strength.

Yu et al. [26] investigated Ka-series with a 19A duct by employing panel method and RANS code and concluded that RANS code produces better result. Szafran et al. [22] studied the effects of duct shape on ducted propeller and concluded that between conventional 19A nozzle and perspective NACA-73_4212 nozzle, 19A nozzle gives better performance. Razaghian and Ghassemi [19]analyzed a conventional propeller and then same propeller was fitted with accelerating 19A and decelerating N32 duct. 19A duct improved propeller characteristics while N32 model had a negative effect at lower advance coefficient. In the study of Majdfar et al. [12] about the effect of length and angle of 19A duct on the hydrodynamic performance of propeller found that increase in duct length doesn't significantly change the thrust coefficient. Gaggero et al. [8] designed ducted propeller with a decelerating type of duct and found reduce cavitation phenomenon. Du and Kinnas [3] analyzed Ka4-70 propeller with a19A duct. Target thrust is achieved with a higher efficiency after a few iterations by coupling RANS code with nonlinear optimization method.

The research mentioned above mainly focused on numerical analysis of either conventional marine propeller or ducted propeller. For this purpose, they applied RANSE code and other CFD methods on different types of propellers and duct. Various type of elements is used such as Tetrahedral, Quadrilateral, Hexahedral and so on. Different mesh size and grid independence test is also carried out to produce accurate result. In most cases researchers have used small size prototype propeller for simulation purpose and validate their result by towing tank experiment or by already published experimental data. These studies play an

important role for further research using RANSE method to predict propeller open water characteristics. However, their focus was not on how conventional and ducted propeller performance varies over advance coefficient under same set of constraints. Moreover, they hardly consider the effect of fluid flow around an actual ship size propeller and its time complexity for simulation.

In this research, an actual size three bladed Wageningen B-series propeller is designed in an iterative process. After geometric modeling of the propeller, it is numerically analyzed using commercial ANSYS CFX software. The same propeller is then fitted with an accelerating 19A duct and numerically analyzed again.

2.0 THEORETICAL FRAMEWORK

The thrust and torque coefficient of the Wageningen B-series propeller is expressed by following regression formulae.

$$K_T = \sum_{n=0}^{39} C_n (J)^{S_n} \left(\frac{P}{D}\right)^{t_n} \left(\frac{A_E}{A_0}\right)^{u_n} (Z)^{v_n} \quad \dots (1)$$

$$K_Q = \sum_{n=0}^{47} C_n (J)^{S_n} \left(\frac{P}{D}\right)^{t_n} \left(\frac{A_E}{A_0}\right)^{u_n} (Z)^{v_n} \quad \dots (2)$$

2.1 Hydrodynamic Coefficient

Whenever a propeller with a diameter (D) rotates in a uniform flow with angular velocity ($\omega = 2\pi n$) and velocity of advance (V_A) it generates thrust and torque. The hydrodynamic characteristics of a propeller are the non-dimensional coefficients that describe the forces and moments acting on the propeller. These coefficients are the advance coefficient (J), the propeller thrust coefficient (K_T), torque coefficient (K_Q) and open water efficiency (η_0) which can be computed respectively as follows:

$$J = \frac{V_A}{n \cdot D}; \quad K_T = \frac{T}{\rho \cdot n^2 \cdot D^5} \quad \dots (3)$$

$$K_Q = \frac{Q}{\rho \cdot n^2 \cdot D^5}; \quad \eta_0 = \frac{J}{2\pi} \cdot \frac{K_T}{K_Q} \quad \dots (4)$$

Where, T and Q are thrust and torque of the propeller.

2.2 Governing Equation of Fluid Flow

The fluid is assumed to be incompressible. The three-dimensional flow of incompressible viscous fluid can be described by the equations as follows:

- Continuity equation

$$\frac{\partial p}{\partial t} + \frac{\partial(\rho u_x)}{\partial x} + \frac{\partial(\rho u_y)}{\partial y} + \frac{\partial(\rho u_z)}{\partial z} = 0 \quad \dots (5)$$

- Conservation of momentum equation

$$\rho\left(\frac{\partial V}{\partial t} + V \cdot \nabla V\right) = -\nabla p + \mu \nabla^2 V + \rho g \quad \dots (6)$$

- Equation of Turbulent Kinetic Energy

$$\frac{\partial(\rho k)}{\partial t} + \frac{\partial(\rho k u_i)}{\partial x_i} = \frac{\partial}{\partial x_j}\left[\left(\mu + \frac{\mu_t}{\sigma_k}\right) \cdot \frac{\partial k}{\partial x_j}\right] + P_k + P_b - \rho\epsilon - Y_M + S_k \quad \dots (7)$$

- Equation of Energy Dissipation

$$\frac{\partial(\rho \epsilon)}{\partial t} + \frac{\partial(\rho \epsilon u_i)}{\partial x_i} = \frac{\partial}{\partial x_j}\left[\left(\mu + \frac{\mu_t}{\sigma_k}\right) \cdot \frac{\partial \epsilon}{\partial x_j}\right] + C_{1\epsilon}\frac{\epsilon}{k}(P_k + C_{3\epsilon}P_b) - C_{2\epsilon}\rho\frac{\epsilon^2}{k} + S_\epsilon \quad \dots (8)$$

3.0 NUMERICAL SIMULATION

The numerical model already presented is applied on a three-bladed conventional propeller. Before the application of numerical code geometry of the propeller and duct must be created properly.

3.1 Geometric Modelling

The propeller adopted here is the Wageningen B-series propeller. Optimal diameter and pitch ratio of the propeller for the given power and propeller rpm are found 1.82m and 0.76 respectively through an iteration process using Eq. (1) and Eq.(2). Optimum value of advance coefficient is found as 0.36. The coordinates of the Wageningen-B series propeller for the chosen design are calculated [10]. Using the coordinates, 3D geometry is constructed in the plotting software PropCad. It has made the geometry generation easier by considering easy setup of rake and skew angle. Again, this 3D geometry is further modified in software Rhinoceros for joining of the blades and hub, smothering of the joints etc.

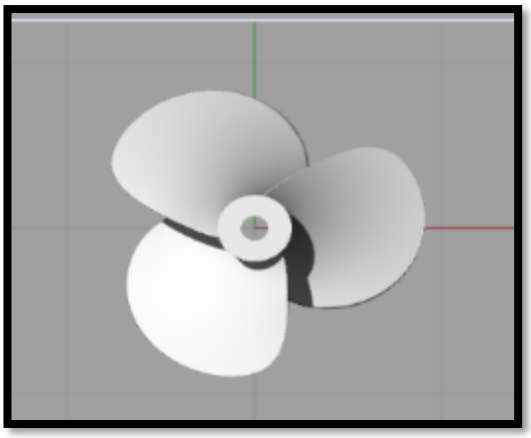

1(a): 3D propeller model(conventional)

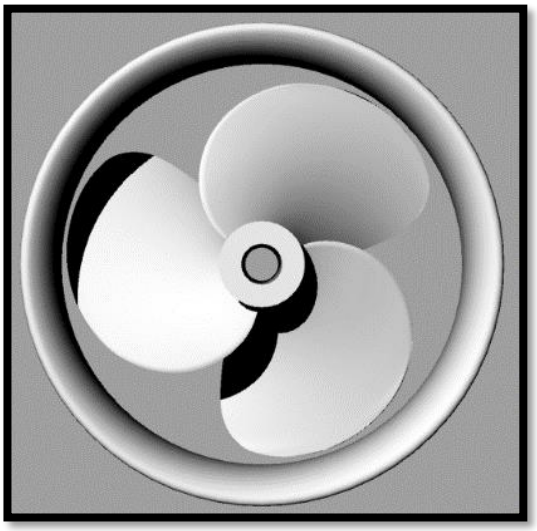

1(b): 3D propeller model (Ducted)

Figure 1: 3D model of conventional and ducted propeller

3.2 Mesh Generation and Boundary Condition

Discretization of the rotary and static domain is done by FVM (Finite Volume Method). The domain sizes are specified in Figure 2.

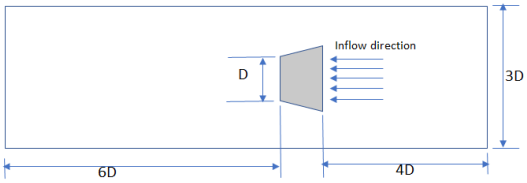

Figure 2: Scheme for propeller and fluid domain

The Mesh element is tetrahedral. Both global and local meshing has been done. Local meshing has been applied at the propeller (in case of the ducted propeller in duct too) with a smaller cell size due to the complex shape of propeller to get better results. Quadratic order element, curvature capture (Minimum size: 10mm, Normal angle: 20˚), proximity capture (Minimum size: Globally 10mm and locally 5mm), Inflation (Maximum layer: 5, Growth rate: 1.2), Pitch tolerance (9mm), patch conforming method have been applied here. At global meshing, the element size is 200mm and it is 20mm at local meshing. Mesh convergence test has been performed for the conventional propeller.

Table 1: Mesh sensitivity analysis

Element size (mm)	Total number of elements	% Error in K_T	% Error in $10K_Q$	% Error in η_0
15	1910315	4.4117	9.7078	5.8655
20	1677098	4.1578	10.0726	6.5773
25	1586888	3.7780	10.3093	7.2821
30	1546380	3.9821	10.7350	7.5650
40	1515127	3.8470	11.0408	8.0867
60	1502253	3.7629	11.1956	8.3698

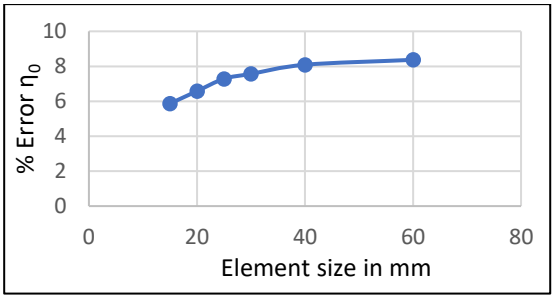

Figure 3: Mesh convergence

Reduction in size of the element reduces the error percentage of open water efficiency. The least percentage of error is observed in element size 15mm, but the simulation time is greater than other element sizes. Since the result does not vary significantly after reduction of element size below 25mm, 20mm element size has been chosen for simulation since it gives quite reasonable error percentage in reasonable simulation time. For the conventional propeller system, the total number of elements is 1677098 and total number of nodes is 2341817. For the ducted propeller system, the total number of elements is 3180289 and total number of nodes is 4474012. The meshing view of the conventional and ducted systems are shown in Figure 4.

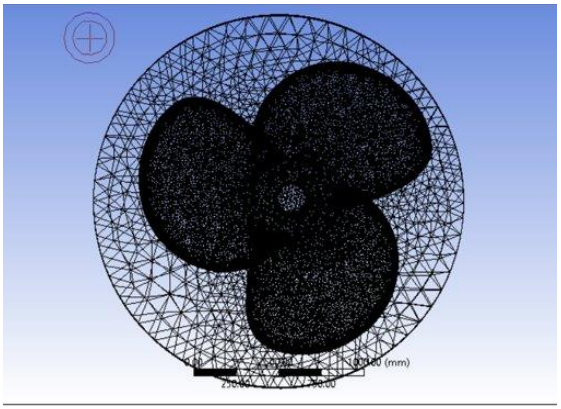

4(a): Conventional propeller meshing

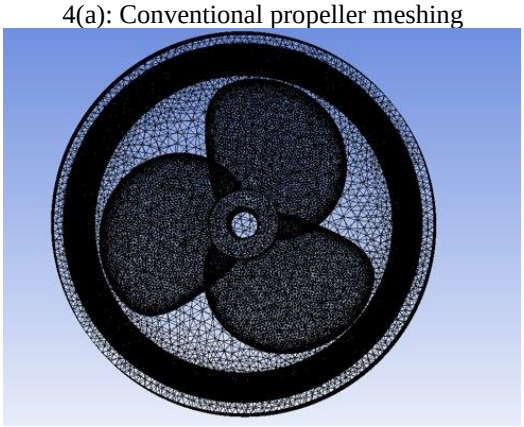

4(b): Ducted propeller meshing

Figure 4: Meshing of conventional and ducted propeller

Three types of boundary conditions used here. They are the velocity inlet, pressure outlet and taking the propeller surface as Stationary Wall with No slip Shear condition. In case of ducted propeller, the duct is on no slip wall boundary condition.

3.3 Solver Settings

The applied CFD code is ANSYS CFX. The RANS solver used here is pressure based with implicit formulation of linearization. The velocity formulation type is absolute not relative and flow condition is not steady but transient. The viscous effect is considered as the $k-\epsilon$ relializable turbulent model is used. In the fluid zone, the frame motion has been applied where the propeller is stationary and the fluid will move rotating at an angular speed of 393 rpm. This is also referred as moving reference frame. SIMPLE algorithm has been chosen as the pressure-velocity method. Discretization method for pressure is second order and for momentum it is turbulent kinetic energy, turbulent dissipation rate is second order upwind. Hybrid Initialization has been chosen as the initialization method. In case of ducted propeller, instead of frame motion mesh motion is applied. Number of iterations and remaining amount varies simulation to simulation.

4.0 RESULTS AND DISCUSSION

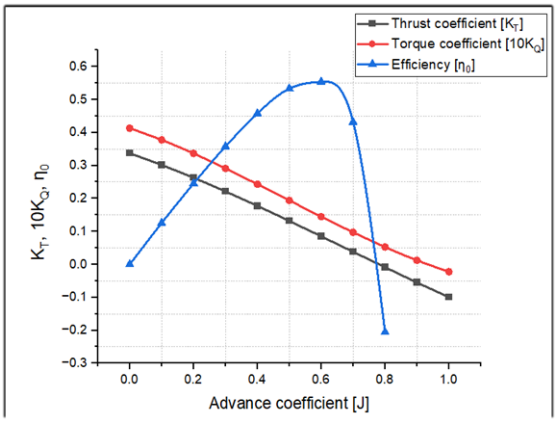

Figure 5: Open water diagram of conventional propeller (Regression)

Open water diagram is plotted based on the data obtained from polynomial regression of Wageningen-B series propeller as shown in Figure 5. Regression result shows that after $J = 0.7$ thrust of conventional propeller become negative and maximum efficiency is $\mathbf{56}\%$ (approx.). Numerical analysis has been performed on this propeller and open water diagram is plotted using the data obtained from numerical analysis as shown in Figure 6.

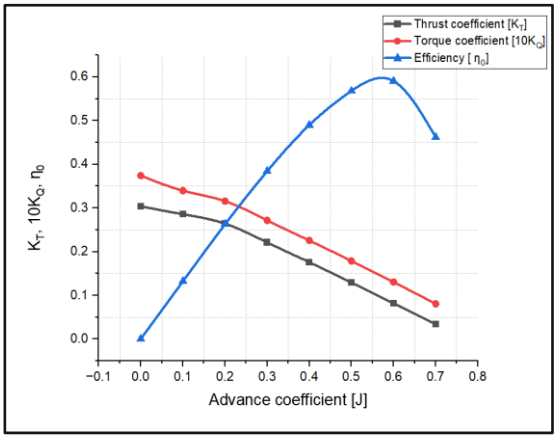

Figure 6: Open water diagram of conventional propeller (Numerical)

Numerical result also shows that thrust is negative after J = 07. It provides a maximum efficiency of 60% (approx.). A comparison has been made between regression and numerical result in terms of percentage difference as shown in Table 2.

Table 2:Percentage difference between Theoretical and Numerical Analysis

J	$\%K_T$	$\% \ 10K_Q$	$\%\eta_0$
.0001	9.8590	9.4799	0.4188
0.1	3.5041	8.4616	-5.4157
0.2	-0.4950	6.1777	-7.1121
0.3	-0.0224	6.8123	-7.3344
0.4	0.8051	7.3060	-7.0133
0.5	2.0277	8.0236	-6.5189
0.6	4.1578	10.0726	-6.5773
0.7	11.4879	17.1998	-6.8984
0.8	-100.6801	50.4272	-304.818
0.9	-41.5465	414.5264	145.0031
1	-52.5393	-429.479	71.1907

The analysis is focused on advance coefficient up to J = 0.6. Within this range Table 2 indicates an acceptable level of percentage of error. In some cases, the percentage errors are even lower than 1%. A graphical representation of this comparison is shown in Figure 7.

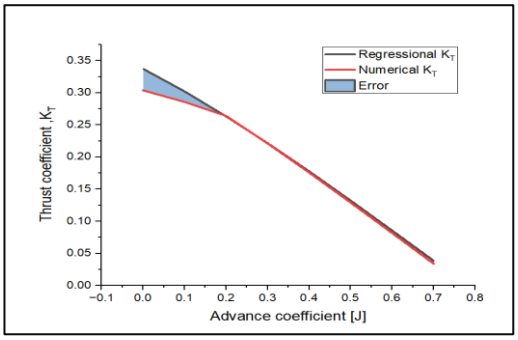

7(a): Error in thrust coefficient

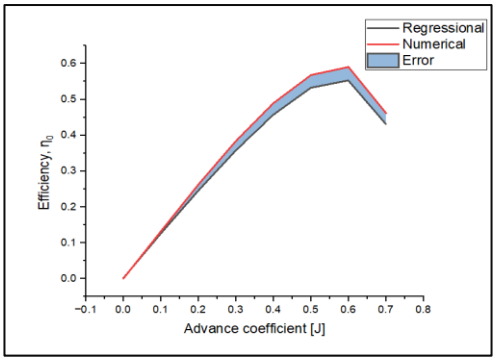

7(b): Error in efficiency

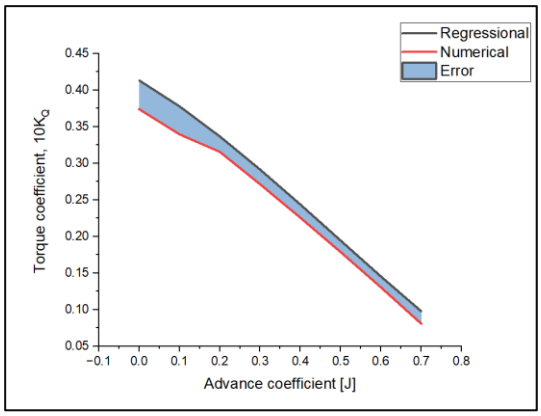

7(c): Error in torque coefficient

Figure 7: Comparison of Numerical Analysis with Theoretical Result

From the above comparison, it can be concluded that the efficiency obtained from the numerical result is giving slightly higher values than the regression result. The percentage error in thrust is much lower than error in torque and efficiency. Error percentage corresponding to the optimum advance coefficient is 7.14%.

Table 3: Error percentage for optimum value

J	0.3	.36	.4
$\% \ K_T$	0.02	.49	.81
$\% \ K_Q$	6.81	7.11	7.31
$\% \ \eta_0$	7.33	7.14	7.01

Ducted Propeller

Numerical analysis of ducted propeller shows that the thrust of the duct becomes negative from $J = 0.5$ which means as the speed increases, the performance of the duct decreases.

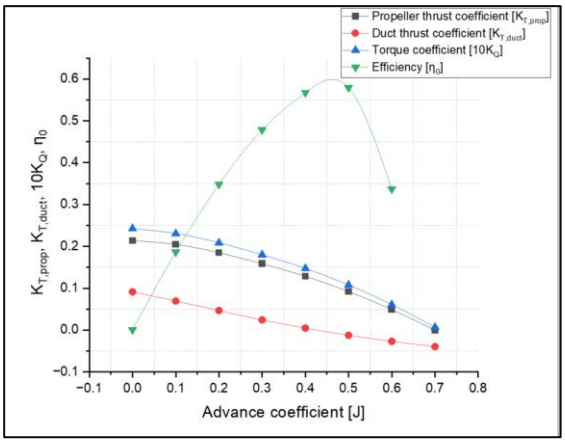

Figure 8: Open water diagram of ducted propeller

Figure 8 shows that optimum efficiency is approximately 60% and the thrust of the propeller

is always higher than the thrust of the duct. Furthermore, a comparison of efficiency has been made between the numerical results of the conventional propeller and ducted propeller as shown in Figure 9.

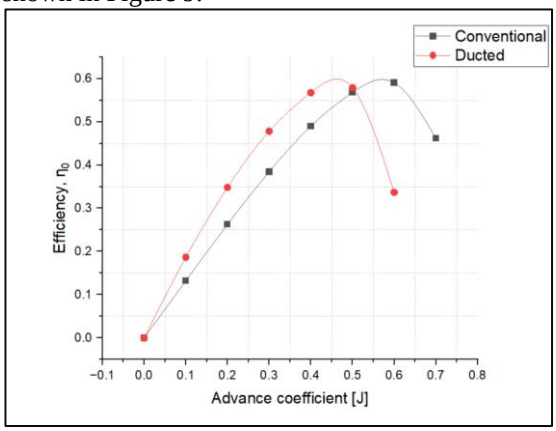

Figure 9: Comparison between conventional and ducted propeller

This comparison shows that efficiency of ducted propeller increases as the advance coefficient increases. Efficiency of ducted propeller is highest at $J = 0.48$ (approx.) and service speed corresponding to this advance coefficient is 13 knots. For service speed higher than 13 knots, efficiency of the ducted propeller decreases significantly. Efficiency curves of ducted and conventional propeller intersect at $J = 0.5$ and service speed corresponding to this advance coefficient is 14 knots. For service speed above 14 knots, conventional propeller provides higher efficiency than ducted propeller. Therefore, both conventional and ducted propeller can be useful depending on the service speed of a particular vessel.

5.0 CONCLUSIONS

In this paper, conventional propeller as well as ducted propeller were analyzed at different advance coefficient. Based on the numerical results following conclusions can be drawn.

- The open water characteristics of the conventional propeller are almost similar in case of regression and numerical analysis and there is on an average 5.92% of error in efficiency.
- Both the conventional and ducted propeller systems have the highest efficiency of around 60% but at different speeds.
- The ducted system provides better efficiency up to $J = 0.48$ and after that the conventional system provides better performance. This conclusion can be drawn with more certainty if the ducted propeller can be tested in a towing tank or if numerical results can be verified by previously published experimental data.
- Accurate estimation of propeller hydrodynamic characteristics using CFD largely depend on turbulence model, selected mesh type and mesh density. $k - \epsilon$ Realizable model with tetrahedral meshes of reasonable size have the ability to produce better result.
- The numerical results are intended to be more accurate estimates than prototype model tests since an actual size propeller is simulated. The propeller performance is influenced by a variety of factors such as the effect of hull form, engine propeller matching and fouling after certain operational period etc. So actual performance of a propeller can only be known after fully loaded service condition.

In future various RANSE solver, different types of propellers and duct geometry can be studied. Additionally, if facility to experiment is accessible, towing tank experiment can also be done to verify the results of simulation.

ACKNOWLEDGEMENT

We are thankful to Department of Naval Architecture and Marine engineering of BUET for providing necessary resources of this research project. The authors would like to thank anonymous reviewers for providing suggestions which improved the quality of this article.

REFERENCES

[1] Bahatmaka, A., Kim, D. J., & Zhang, Y. (2018). Verification of cfd method for meshing analysis on the propeller performance with openfoam. In *2018 International Conference on Computing, Electronics & Communications Engineering.*

[2] Boumediene, K., Belhenniche, S., Imine, O., & Bouzit, M. (2019). Computational hydrodynamic analysis of a highly skewed marine propeller. *Journal of Naval Architecture and Marine Engineering*, *16*(1), 21-32.

[3] Du, W., & Kinnas, S. A. (2019, June). Optimization Design and Analysis of Marine Ducted Propellers by RANS/Potential Flow Coupling Method. In *The 29th International Ocean and Polar Engineering Conference*, *OnePetro.*

[4] DurgaNeeharika, P., & Babu, P. S. (2015). Design and analysis of ship propeller using FEA. In *Proceedings of International Conference on Recent Trends in Mechanical Engineering*.

[5] Elghorab, M. A., Aly, A. A. E. A., Elwetedy, A. S., & Kotb, M. A. (2013). Open Water Performance Marine Propellers Using CFD. *Research Gate*.

[6] Fitriadhy, A., Adam, N. A., Quah, C. J., Koto, J., & Mahmuddin, F. (2020). CFD prediction of b-series propeller performance in open water. *CFD Letters*, *12*(2), 58-68.

[7] Funeno, I. (2002). On Viscous Flow around Marine Propellers-Hub Vortex and Scale Effect. *Journal of the Kansai Society of Naval Architects, Japan*, *2002*(238), 17-27.

[8] Gaggero**,** S., Rizzo, C. M., Tani, G., & Viviani, M. (2012). EFD and CFD design and analysis of a propeller in decelerating duct. *International Journal of Rotating Machinery*.

[9] Harish, B., Prasad, K. S., & Rao, G. U. M. (2015). Static Analysis of 4-Blade Marine Propeller. *Journal of Aerospace Engineering & Technology*, *5*(2).

[10] https://github.com/zlaku72/Propeller_Analysis

[11] Kolakoti, A., Bhanuprakash, T. V. K., & Das, H. N. (2013). CFD analysis of controllable pitch propeller used in marine vehicle. *Global Journal of Engineering Design and Technology*, *2*(5), 25-33

[12] Majdfar, S., Ghassemi, H., Forouzan, H., & Ashrafi, A. (2017). Hydrodynamic prediction of the ducted propeller by CFD solver. *Journal of Marine Science and Technology*, *25*(3), 3.

[13] Marti nez-Calle, J. N., Balbona-Calvo, L., Gonza lez-Pe rez, J., & Blanco-Marigorta, E. (2002). An open water numerical model for a marine propeller: A comparison with experimental data. In *Fluids Engineering Division Summer Meeting*, 36(169), 807-813.

[14] Midoro, R., Musso, E., & Parola, F. (2005). Maritime liner shipping and the stevedoring industry: market structure and competition strategies. *Maritime Policy & Management*, *32*(2), 89-106.

[15] Mosaad, M. A., MM, H., & Yehia, W. (2011). Guidelines for numerical flow simulation around marine propeller. In *First International Symposium on Naval Architecture and Maritime, Istanbul*.

[16] Parra, C. (2013). Numerical investigation of the hydrodynamic performances of marine propeller. *University of Galati, Gdynia, Master's thesis*.

[17] Perali, P., Lloyd, T., & Vaz, G. (2016). Comparison of uRANS and BEM-BEM for propeller pressure pulse prediction: E779A propeller in a cavitation tunnel. In *Proceedings of the 19th Numerical Towing Tank Symposium, Nantes, France*.

[18] Prakash, S., & Nath, D. R. (2012). A computational method for determination of open water performance of a marine propeller. *International Journal of Computer Applications*, *58*(12).

[19] Razaghian, A. H., & Ghassemi, H. (2016). Numerical analysis of the hydrodynamic characteristics of the accelerating and decelerating ducted propeller. *Zeszyty Naukowe Akademii Morskiej w Szczecinie*, 47 (119), 42-53.

[20] Saha, G. K., Maruf, M. H. I., & Hasan, M. R. (2018). Marine propeller design using CFD tools. *The Institution of Engineers, Bangladesh*, 64.

[21] Shreyash C. G., Aditya M. P., Shashank P. S. & Dheeraj K. A. (2020). Performance Analysis and Enhancement of Marine Propeller, *international journal of engineering research & technology*, 09(02).

[22] Szafran, K., Shcherbonos, O., & Ejmocki, D. (2014). Effects of duct shape on ducted propeller thrust performance. *Prace Instytutu Lotnictwa*.

[23] Trejo, I., Terceno, M., Valle, J., Iranzo, A., & Domingo, J. E. R. O. N. I. M. O. (2007). Analysis of a ship propeller using cfd codes. *Calculation of the resistance and the wave profile*.

[24] Triet, P. M., Thien, P. Q., & Hieu, N. K. (2018). CFD simulation for the Wageningen B-Series propeller characteristics in open-water condition using k-epsilon turbulence model. *Science & Technology Development Journal-Engineering and Technology*, *1*(1), 35-42.

[25] Watanabe, T., Kawamura, T., Takekoshi, Y., Maeda, M., & Rhee, S. H. (2003, November). Simulation of steady and unsteady cavitation on a marine propeller using a RANS CFD code. In *Proceedings of The Fifth International Symposium on Cavitation.*

[26] Yu, L., Greve, M., Druckenbrod, M., & Abdel-Maksoud, M. (2013). Numerical analysis of ducted propeller performance under open water test condition. *Journal of marine science and technology*, *18*(3), 381-394.